

Heavy and light chain homologs of ferritin are essential for blood-feeding and egg production of the ectoparasitic copepod *Lepeophtheirus salmonis*

Erna Irene Heggland^{a,*}, Christiane Tröbe^b, Christiane Eichner^a, Frank Nilsen^a

^a Department of Biological Sciences & Sea Lice Research Centre (SLRC), University of Bergen, Norway

^b Department of Biological Sciences, University of Bergen, Norway

ARTICLE INFO

Keywords:

Salmon louse
Blood-Feeding
Knockdown
Starvation
Iron
Ferritin

ABSTRACT

The salmon louse, *Lepeophtheirus salmonis*, is a hematophagous ectoparasite of salmonid fish. Due to its blood-feeding activity, the louse is exposed to great amounts of iron, which is an essential, yet potentially toxic mineral. The major known iron storage protein is ferritin, which the salmon louse encodes four genes of (*LsFer1-4*). Two of the ferritins are predicted to be secreted. These are one of the heavy chain homologs (*LsFer1*) and the light chain homolog (*LsFer2*). Here, we perform functional studies and characterize the two secreted ferritins. Our results show that knocking down *LsFer1* and *LsFer2* both negatively affect the parasite's physiology, as it is not able to properly feed and reproduce. In a starvation experiment, the transcript levels of both *LsFer1* and *LsFer2* decrease during the starvation period. Combined, these results demonstrate the importance of these genes for the normal parasite biology, and they could thus potentially be targets for pest management.

1. Introduction

Iron is an essential element necessary for many cellular processes in all animals. Iron-containing proteins are present in several key biochemical pathways, such as DNA synthesis, energy metabolism and electron transfer reactions [1]. Free intracellular iron can rapidly be reduced to the ferrous (Fe^{2+}) form, and may catalyze the generation of reactive oxygen species (ROS) which are highly cytotoxic reactive radicals that can cause harm to cellular compounds such as lipids, DNA and proteins [2]. In order to avoid cell harm, iron storage and distribution must be implemented by tightly regulated mechanisms, using designated proteins in the cell.

Ferritin is the major intracellular iron storage protein. Here, ferric iron (Fe^{3+}) is sequestered and kept in a nontoxic, soluble and biologically non-reactive state [3]. In that state, the iron can be recruited to various proteins that require the metal as cofactor to perform their proper biological function. Typically, ferritin is composed of 24 subunits which can harbor up to 4000 Fe atoms [4]. Vertebrate ferritins are made up of the heavy (H) chain and the light (L) chain subunits, whereas arthropod ferritins are made up of homologs to these (heavy-chain homolog, HCH, and light-chain homolog, LCH) which are often secretory [4]. Characteristics for HCH ferritin are amino acid (aa) residues that contribute to a ferroxidase center, which oxidizes Fe^{2+} to Fe^{3+} , tyrosine residues that cause rapid biomineralization of iron, and a

pore opening that allows for iron passage. LCH ferritin is characterized by aa residues that induce nucleation of iron. LCH ferritin often has a larger sequence variety, with less similarity to its vertebrate orthologue, and it is often annotated as LCH because of the lacking ferroxidase center [5]. In contrast to cytoplasmic ferritins, secreted ferritins contain cysteine residues that promote inter- and intrasubunit disulfide bonds [6].

With the exception of intracellular iron within iron storage proteins, the majority of vertebrate iron is found in blood, complexed within the porphyrin ring of heme as a cofactor of hemoglobin used for gas transportation, but also in other forms such as bound to the iron transfer protein transferrin [7]. Blood-feeding parasites ingest high levels of iron and thus need to protect their cells from iron overload upon feeding and absorption. The salmon louse, *Lepeophtheirus salmonis*, is an obligate marine ectoparasite, feeding off the skin and blood of its salmonid fish host [8]. With an increasing resistance towards various chemical treatments [9], the salmon louse is considered to be an economically and ecologically important parasite to combat. The parasite's life cycle is divided into eight stages which are as follows: the planktonic nauplius I and II, the infectious copepodid, the attached parasitic chalimus I and II, and the mobile parasitic preadult I and II and adult lice [10,11]. At 10 °C, the development of *L. salmonis* from fertilization to mature adult lice is completed in approximately 40 (male) to 52 (female) days [12]. Once the female louse has reached the mature adult

* Corresponding author at: University of Bergen, Thormøhlensgate 53 A/B, 5020, Bergen, Norway.

E-mail address: Erna.Heggland@uib.no (E.I. Heggland).

<https://doi.org/10.1016/j.molbiopara.2019.111197>

Received 15 May 2019; Received in revised form 13 June 2019; Accepted 19 June 2019

Available online 25 June 2019

0166-6851/ © 2019 The Authors. Published by Elsevier B.V. This is an open access article under the CC BY license (<http://creativecommons.org/licenses/by/4.0/>).

stage, it will continuously produce pairwise egg strings. The hatching larvae have the potential to further infect hosts upon reaching the copepodid stage. In order to be able to successfully produce viable offspring, the louse needs to absorb several macro- and micronutrients from its blood meal. One of the many micronutrients required for oocyte development is the mineral iron, which the salmon louse requires proper storage for until it is needed in iron-proteins.

Here, we report the presence of four ferritin homologs (*LsFer1-4*) in the genome of *L. salmonis* and analyze the sequences. Further, we perform functional studies of the two ferritins with signal peptides (*LsFer1* and *LsFer2*) by *in situ* hybridization, starvation as well as RNA interference (RNAi) to evaluate the importance of these genes in reproduction and blood-feeding of the adult female salmon louse. Results from the knockdown study illustrate the detrimental effects for the hematophagous parasite lacking *LsFer1* or *LsFer2*, as normal development and fecundity is negatively impacted upon RNAi mediated knockdown of the genes.

2. Material and methods

2.1. Sequence analyses

Initial data for searching transcript and protein sequences and primer design were extracted from the *L. salmonis* genome annotation in Ensembl Metazoa (https://metazoa.ensembl.org/Lepeophtheirus_salmonis). All following analyses are based on the GenBank sequences: *BT121711* (*LsFer1*), *BT121232* (*LsFer2*), *MK887318* (*LsFer3*), *BT077723* (*LsFer4a*) and *BT121164* (*LsFer4b*). Glycosylation prediction was performed using the NetNGlyc 1.0 Server (<http://www.cbs.dtu.dk/services/NetNGlyc/>) and the NetOGlyc 4.0 Server [13]. Protein BLAST searches were conducted against the Genbank and SwissProt databases [14]. Conserved domain search was conducted using InterProScan [15]. Signal peptides and cleavage sites in the aa sequences were predicted using Phobius [16]. Searches for iron-responsive elements (IREs) in the untranslated regions were performed using SIREs Web Server 2.0 [17].

2.2. Sequence alignment and phylogeny

Aa sequences of *LsFer1-4* were used to obtain ferritins of various species from a BLASTp search [14] or from searching The UniProt Consortium [18] for ferritins of model organisms. Alignment was performed in UGENE using MUSCLE alignment under default conditions [19,20]. Grey shading indicates percentage identity. For alignment, following sequences annotated with heavy chain were chosen: *Homo sapiens* (UniProt: P02794), *Salmo salar* (UniProt: P49946), *Xenopus laevis* (UniProt: P49948), *Caenorhabditis elegans* (NP_491198.1), *Penaeus monodon* (ABP68819.1), *Haemaphysalis longicornis* (AAQ54713.1), *H. longicornis* (BAN13552.1)*, *Trichoplusia ni* (XP_026744300.1)*, *Manduca sexta* (AAK39636.1)*, *Anopheles gambiae* (XP_312474.4)*. Light chain sequences chosen were: *H. sapiens* (UniProt: P02792), *X. laevis* (UniProt: Q7SXA5), *S. salar* (NP_001134896.1), *T. ni* (XP_026744299.1)*, *M. sexta* (AAF44717.1)*, *A. gambiae* (XP_001237468.3)*. Sequences with signal peptides are marked with *. For alignment however, the signal sequence was removed. From sequences without signal peptides, the start methionine was removed for alignment.

Sequences used for phylogenetic analysis were: *Caligus clemensi* (ACO15165.1 and ACO14799.1), *Caligus rogercresseyi* (ACO11534.1), *Drosophila melanogaster* (AAF07876.1, NP_524873.1 and NP_572854.1), *Aedes aegypti* (AAO41698.1 and AQY17412.1), *Ixodes ricinus* (ACJ70653.1), *Rhipicephalus microplus* (UniProt: A0A034WXT0), *S. salar* (UniProt: P49947 and P49946), *H. sapiens* (UniProt: P02792 and P02794), *Mus musculus* (UniProt: P29391 and P09528), *C. elegans* (NP_504944.2 and NP_491198.1) and *H. longicornis* (BAN13552.1 and AAQ54713.1). The website <http://www.phylogeny.fr> was used to construct the phylogenetic tree with default settings [21]. More

specifically, sequences were adjusted and aligned by MUSCLE with defaults [20]. The phylogenetic tree was reconstructed by maximum likelihood in PhyML using WAG + G model [22]. The graphical tree was obtained using TreeDyn [23].

2.3. Animals

L. salmonis salmonis was raised on Atlantic salmon (*S. salar*) under laboratory conditions in tanks with seawater (salinity 34.5 ppt and 10 °C) as described before [24]. Fish were daily handfed commercial dry pellets and kept according to Norwegian animal welfare regulations. Experiments were approved by the governmental Norwegian Animal Research Authority (ID8589). Fish carrying lice from RNAi experiments were kept in single-fish tanks [25]. Fish were anesthetized with a mixture of methomidate (5 mg/l) and benzocaine (60 mg/l) upon samplings, or setup of salmon louse infections. Egg string pairs with larvae were incubated and hatched in single incubators in a sea-water flow through system [24].

2.4. Ontogeny

The genomic location for the validated transcript sequences (RACE-PCR) were determined using the software GMAP [26] with the Atlantic salmon louse genome (LSalAtl2s, https://metazoa.ensembl.org/Lepeophtheirus_salmonis) and the raw reads of existing RNA-sequencing data were recounted by *featureCounts* [27] at these regions. Available RNA-sequencing data are used as found in LiceBase (<http://licebase.org>, Dondrup et al., in prep) and from data of a time-series previously published [28]. Data from LiceBase are bulk samples of different developmental stages (nauplius I, nauplius II, planktonic copepodids, attached copepodids at three different sampling time points, chalimus I and II, female and male of preadult I and II and adult lice, as well as eggs (unfertilized extracted from the genital complex of the adult female, immature fertilized eggs (0–24 hours after extrusion) and more mature fertilized eggs (2–7 days after extrusion)). In addition, samples of different tissues (intestine, ovaries, testis feet and antenna) are shown. The data from the time series [28] are RNA-sequencing samples of attached parasitic stages (chalimus I and II and preadult I), which were divided into different instar ages (called young (directly after previous molt), middle and old (directly before next molt)) as well as planktonic copepodids. In addition, unpublished RNA-sequencing data (Eichner et al., unpublished) for the transcript regions from nauplius I and II, taken at three different time points (directly after hatching or molting respectively, in the middle of the stage, and before the next molt) as well as attached copepodids, sampled one, three and five days after infection, are included. RNA-sequencing and data processing for the nauplius and attached copepodid samples was done using the same protocols as in Eichner et al. [28]. Six biological replicates were sequenced for each time point. Normalization was done by edgeR [29] after combining all data sets using the same protocol as in Eichner et al. [28].

2.5. Isolating RNA, synthesis of cDNA, qRT-PCR and RACE

Tissues for RNA isolation were stored in RNAlater (Ambion), at 4 °C overnight and then at –20 °C until usage. Total RNA extraction from adult female lice was executed using TRI Reagent (Sigma-Aldrich) as instructed by the manufacturer. Samples were homogenized using 5 mm stainless steel beads and a TissueLyser II (Qiagen) for 1 min at 30 Hz. Genomic DNA digestion was done by DNase I after manufacturer's instructions (Invitrogen). Quantification of RNA and purity check were done using NanoDrop ND-1000 UV–vis Spectrophotometer (NanoDrop Technologies). DNase-treated RNA was reverse transcribed using the AffinityScript QPCR cDNA Synthesis Kit (Stratagene). qRT-PCR was performed on a QuantStudio 3 qPCR machine using PowerUp SYBR Green Master Mix (Applied Biosystems) on duplicate samples

Table 1

Primers used for RACE, *in situ* hybridization (ISH), RNA interference (RNAi) and qPCR. T7 promoter extension is underlined. Primer efficiency (E%) is given for qPCR assays.

Primer name	Sequence (5'→3')	Application/E%
<i>LsFer1</i> 5' RACE	TCCAGTCACCAAGGCCTCATG	5' RACE
<i>LsFer1</i> 3' RACE	GCAAGATTATCTCTCTGGAGATTGGC	3' RACE
<i>LsFer2</i> 5' RACE	GTATTTGGTCTTGTCATTCGGGGC	5' RACE
<i>LsFer2</i> 3' RACE	GGTGCTCACACTGATGTACAATGTGG	3' RACE
<i>LsFer3</i> 5' RACE	CACGCCCTGGTCCAACACGTTTCATT	5' RACE
<i>LsFer3</i> 3' RACE	CAAGCATGGCTCAACAATCCAGC	3' RACE
<i>LsFer4</i> 5' RACE	ACGAGTTAAGAGGGTTCCAA	5' RACE
<i>LsFer4</i> 3' RACE	ATGAGTTCCCAAATCCGTCA	3' RACE
<i>LsFer1</i> T7 fwd	<u>TAATACGACTCACTATAGGGACAGGAGCCCATGGATCTTGTA</u>	ISH/RNAi
<i>LsFer1</i> rev	TCCAGTCACCAAGGCCTCATG	ISH/RNAi
<i>LsFer1</i> T7 rev	<u>TAATACGACTCACTATAGGGTCCAGTCACCAAGGCCTCATG</u>	ISH/RNAi
<i>LsFer2</i> fwd	GGTGCTCACACTGATGTACAATGTGG	ISH/RNAi
<i>LsFer2</i> T7 fwd	<u>TAATACGACTCACTATAGGGGTGCTCACACTGATGTACAATGTGG</u>	ISH/RNAi
<i>LsFer2</i> rev	GTATTTGGTCTTGTCATTCGGGGC	ISH/RNAi
<i>LsFer2</i> T7 rev	<u>TAATACGACTCACTATAGGGGTATTTGGTCTTGTCATTCGGGGC</u>	ISH/RNAi
Cod_CPY185 fwd	<u>TAATACGACTCACTATAGGGATAGGGCGAATTGGGTACCG</u>	RNAi
Cod_CPY185 rev	<u>TAATACGACTCACTATAGGGAAAAGGGAACAAAAGCTGGAGC</u>	RNAi
SYBR <i>LsEF1α</i> fwd	GGTCGACAGACGTACTGGTAAATCC	qPCR/93%
SYBR <i>LsEF1α</i> rev	TGCGGCCCTTGGTGGTGGTTC	qPCR
SYBR <i>LsFer1</i> fwd	GCAAGATTATCTCTCTGGAGATTGGC	qPCR/93%
SYBR <i>LsFer1</i> rev	TCCAGTCACCAAGGCCTCATG	qPCR
SYBR <i>LsFer2</i> fwd	GGTGCTCACACTGATGTACAATGTGG	qPCR/92%
SYBR <i>LsFer2</i> rev	CAAATGTCTGTTGATAAGAACCAGAG	qPCR

(PCR: 50 °C for 2 min, 95 °C for 2 min, 40 cycles of 95 °C for 15 s and 60 °C for 1 min, and finally a melt curve analysis at 60–95 °C). Duplicate samples had a difference in Ct-values less than 0.35. The reference gene *LseEF1α* [30] was used to calibrate the *LsFer1* and *LsFer2* transcript levels. A five-point standard curve of twofold dilutions was prepared to test the efficiency of the qPCR assays: $E\% = (10^{1/\text{slope}} - 1) \times 100$ [31]. Relative differences ($\Delta\Delta C_t$) in threshold were calculated and transformed by the formula $2^{-\Delta\Delta C_t}$ [32]. Rapid Amplification of cDNA Ends (RACE) was conducted by using the SMARTer RACE cDNA Amplification Kit (Clontech).

2.6. RNA interference

LsFer1 and *LsFer2* were separately knocked down by RNAi in pre-adult II female lice as described before [33] in two independent experiments. Briefly, double stranded (ds) RNA fragments were synthesized by the Megascript RNAi kit (Ambion) using adult female louse cDNA as template. Atlantic cod (*Gadus morhua*) trypsin (CPY185) fragment was used as negative control. All primers are listed in Table 1. Fragments were diluted to 600 ng/μl and 2% (v/v) bromphenol blue was added to enable visualization of the injections. Preadult II female lice were injected with thin capillaries and left to recover for four hours before being placed on fish in individual tanks (three fish per group with a total of 30–39 female lice). Additionally, an equal number of uninjected adult male lice (in relation to the number of female lice per fish) were also placed on each fish to assess the fecundity of the knockdown animals. Experiments were terminated upon the extrusion of the control lice's second pair of egg strings (approximately 40 days after injection). Upon termination, egg strings were collected and incubated in hatching wells. Any hatching of the egg strings was noted. Adult female lice were sampled in RNAlater for knockdown assessment or in Karnovsky's fixative for histological analyses.

2.7. Histology

Salmon lice destined for histological analyses were fixed in Karnovsky's fixative and sectioned as earlier described [34]. Briefly, 2 μm thick plastic sections were stained with filtered toluidine blue and rinsed with tap water. Ready slides were mounted with DPX mounting solution (Sigma-Aldrich) and covered with glass cover slips.

2.8. In situ hybridization

The localizations of *LsFer1* and *LsFer2* mRNAs were detected in the adult female salmon louse by using *in situ* hybridization (ISH) as earlier described [35,36] with the DIG RNA Labelling Kit (Roche) on two sections per probe. RNA antisense probes of 568 bp (*LsFer1*) and 576 bp (*LsFer2*) were made from a target specific cDNA template (see Table 1 for primer sequences). Sense probes acted as negative control for transcript localizations.

2.9. Starvation

Adult female lice were removed from their host, the Atlantic salmon, and either sampled directly (zero days starved) in RNAlater or placed in individual incubators with running sea water [24]. The lice in the incubators were sampled one, two, four and eight days after being separated from their food source as described before [37]. RNA isolation and cDNA synthesis were performed as described in Section 2.5 on five replicates of each sampling time point. The transcript levels of *LsFer1* and *LsFer2* were finally assessed by qPCR.

2.10. Statistics

Statistics were performed by using IBM SPSS Statistics 23 for Windows. Data sets were first tested by Shapiro-Wilk's test of normality and Levene's test for equality of variances. An independent *t*-test was used to evaluate the mean between two groups. For non-normal data sets, a Mann-Whitney U test was conducted. A *p*-value ≤ 0.05 was considered statistically significant. Data are presented as mean values \pm standard deviations (SD) or as individual values.

3. Results

3.1. Sequence analyses

cDNA sequences of ferritins *LsFer1-4* in the salmon louse were obtained by 5' and 3' RACE using sequence specific primers (Table 1). Main results of sequence analyses are summarized in Table 2. No IREs were predicted for any of the genes. *LsFer1* consists of an open reading frame (ORF) of 639 bp. A protein BLAST search of the *L. salmonis* full

Table 2
Sequence summary of ferritin genes *LsFer1-4* in the salmon louse.

Gene	Signal peptide	Predicted subunit	ORF (including signal peptide)	GenBank ID
<i>LsFer1</i>	Yes	HCH	213 aa	BT121711
<i>LsFer2</i>	Yes	LCH	224 aa	BT121232
<i>LsFer3</i>	No	HCH	180 aa	MK887318
<i>LsFer4a</i>	No	HCH	171 aa	BT077723
<i>LsFer4b</i>	No	HCH	173 aa	BT121164

length *LsFer1* protein showed 78% identity with a Ferritin subunit precursor from *Caligus rogercresseyi* (Genbank accession: [ACO11534.1](#)), 54% identity with Ferritin, lower subunit-like from *Eurytemora affinis* (Genbank accession: [XP_023345228.1](#)), and 40% identity with Ferritin 1-like protein A from *Daphnia pulex* (Genbank accession: [ABK91577.1](#)). *LsFer2* consists of an ORF of 672 bp. A protein BLAST search of the *L. salmonis* full length *LsFer2* protein showed 69% identity with a Ferritin light chain, oocyte isoform from *Caligus clemensi* (Genbank accession: [ACO15165.1](#)), and 29% identity with 32 kDa ferritin subunit from *Galleria mellonella* (Genbank accession: [AAL47694.1](#)). The ORFs of *LsFer1* and *LsFer2* were analyzed in Interpro-Scan, and both proteins were characterized as containing a ferritin-like domain (PF00210). In *LsFer1* there is a predicted ferroxidase site, a ferrihydrite nucleation center and an iron ion channel, which are not predicted in *LsFer2*. *LsFer2* has a predicted dinuclear metal binding motif. A scan in Phobius shows that *LsFer1* has a signal peptide from aa 1 → 21 with a cleavage site from aa 17 → 21, and a non-cytoplasmic region from aa 22 → 213. A Phobius scan for *LsFer2* shows that the protein has a predicted signal peptide from aa 1 → 24 with a cleavage site from aa 17 → 24, and a non-cytoplasmic region from aa 25 → 224. *LsFer1* has two predicted O-linked glycosylation sites at aa 29 and 36 and no predicted N-linked glycosylation sites. *LsFer2* has no predicted O-linked glycosylation site, and one predicted N-linked glycosylation site at aa 55.

LsFer3 has an ORF of 540 bp. A protein blast shows a 59% identity with a ferritin of *Calanus sinicus* (Genbank accession: [APC62655.1](#)) and 58% identity with *Pseudodiaptomus annandalei* (Genbank accession: [AGT28487.1](#)). *LsFer4a* and *b* encode similar ORFs with only slight variations in their C-terminals affecting 3 aas only as well as 2 additional aas in *LsFer4b*. *LsFer4a* has an ORF of 513 bp whereas *LsFer4b* has an ORF of 519 bp. Both *LsFer4a* and *4b* have 60% identity with a ferritin of *Calanus sinicus* (Genbank accession: [APC62655.1](#)) and a 58% identity with a ferritin heavy chain A-like of *Eurytemora affinis* (Genbank accession: [XP_023344839.1](#)). According to Phobius scans, *LsFer3-4* lack signal peptides. Interpro-Scan predicts that *LsFer3-4* have a ferritin-like domain (PF00210) and have ferroxidase activity, a ferrihydrite nucleation center and an iron ion channel.

3.2. Sequence alignment and phylogeny

Sequence alignment (Fig. 1) shows that *LsFer1*, 3, 4a and 4b contain all conserved aas of the ferroxidase site. In addition, the conserved aspartic acid of the iron entry pore is found in all these *L. salmonis* ferritins, while the conserved glutamic acid is not found in *LsFer1*. Like the insect sequences shown in the alignment, it is replaced by threonine. There are only minor differences in the aa sequence between *LsFer4a* and *LsFer4b*, as the nucleotide sequence at the C-terminal end shows differences. *LsFer2* contains only two of the conserved aas making up the functional ferritin motif. However, all of the conserved cysteines found in the light chain of insects responsible for disulfide bridges are also found in *LsFer2*. Two cysteine residues common in disulfide bridges are also conserved in *LsFer1*.

To investigate the relationship between *LsFer1-4* and other vertebrate and invertebrate ferritins, a maximum likelihood phylogenetic analysis was performed (Fig. 2). The analysis shows that *LsFer1* clusters together with secretory invertebrate HCH ferritins. *LsFer2* clusters

together with secretory invertebrate LCH ferritins. Both *LsFer1* and *LsFer2* have their closest relation to ferritin sequences of the parasitic copepod *C. clemensi*. *LsFer3-4* cluster together in a separate clade, close with intracellular ferritins (HC and LC) of both vertebrates and invertebrates.

3.3. Ontogeny

To determine spatial and temporal expression patterns of the ferritin subunits, RNA-sequencing data were used to count the transcripts (Fig. 3). The two secreted ferritins *LsFer1* (Fig. 3a) and *LsFer2* (Fig. 3b) have similar absolute expression counts and pattern, and they are highly expressed in the intestine. *LsFer3* (Fig. 3c) is nearly exclusively found in male lice and transcripts are highly expressed in testis. *LsFer4a* and *LsFer4b* are differing at the 3' end only, and the total count of *LsFer4* is shown (Fig. 3d). *LsFer4* (Fig. 3d) is expressed in the intestine, but is also found in all other tissues investigated, it is highly expressed already in immature eggs.

3.4. In situ hybridization

To localize and confirm where the secretory ferritin transcripts (*LsFer1* and *LsFer2*) are expressed, we utilized *in situ* hybridization. Both transcripts were found to be expressed in cells lining the intestinal tract of the adult female louse (Fig. 4).

3.5. Starvation

To evaluate the effect starvation has on the expression of *LsFer1* and *LsFer2*, transcript levels were measured by qPCR in a time series after removing the lice from their host. With increased time absent from the food source, decreased levels of both transcripts were found in the adult female *L. salmonis* (Fig. 5). More specifically, the expression of *LsFer1* is significantly down-regulated from day 2 and throughout the starvation period (*t*-test: day 1: $p = 0.132$, day 2: $p = 0.001$, day 4: $p = 0.005$, day 8: $p = 0.0000213$, $n = 5$). At eight days of starvation, the expression of *LsFer1* is decreased with on average 67% (Fig. 5a). *LsFer2* shows a similar profile, but shows a significant decrease already from day 1 of starvation (*t*-test: day 1: $p = 0.007$, day 2: $p = 0.0000219$, day 4: $p = 0.0000493$, day 8: $p = 0.00000669$, $n = 5$) and at day 8 of starvation, *LsFer2* has decreased with on average 82% (Fig. 5b).

3.6. RNAi phenotype, histology and knockdown effect of *LsFer1* and *LsFer2*

In order to study the functions of *LsFer1* and *LsFer2* *in vivo*, two independent RNAi knockdown experiments were conducted. In both experiments, the knockdown animals' recovery rates (lice sampled at the end of the experiment/lice injected at the start of the experiment) are similar to the control animals', ranging from 17%–59% (Table 3). However, the fecundity of the parasite is affected by knocking down *LsFer1* or *LsFer2*. In both experiments, larvae from control animals hatched from all egg strings. However, knockdown of *LsFer1* resulted in one hatched out of ten egg string pairs (exp. 1), and when repeated, no egg strings (out of 6 pairs) hatched (exp. 2). Knockdown of *LsFer2* resulted in egg strings present in 10 of 23 animals, and only 5 pairs of these hatched (exp. 1). In experiment 2 of *LsFer2* knockdown, all animals (7 out of 7) had egg strings upon termination, but none of these hatched.

In all control adult female salmon lice, a salmon blood-filled intestinal tract is seen as a red line stretching from the mouth part in the cephalothorax, through the genital segment with maturing oocytes, and finally through the abdomen ending in the rectum (Fig. 6a). When knocking down *LsFer1* (Fig. 6b) and *LsFer2* (Fig. 6c), an alteration in phenotype is seen. In both knockdown groups, the animals have little or no blood in their intestines, as seen by visual inspection (Table 3 and Fig. 6). While all lice in the control groups had a high amount of blood

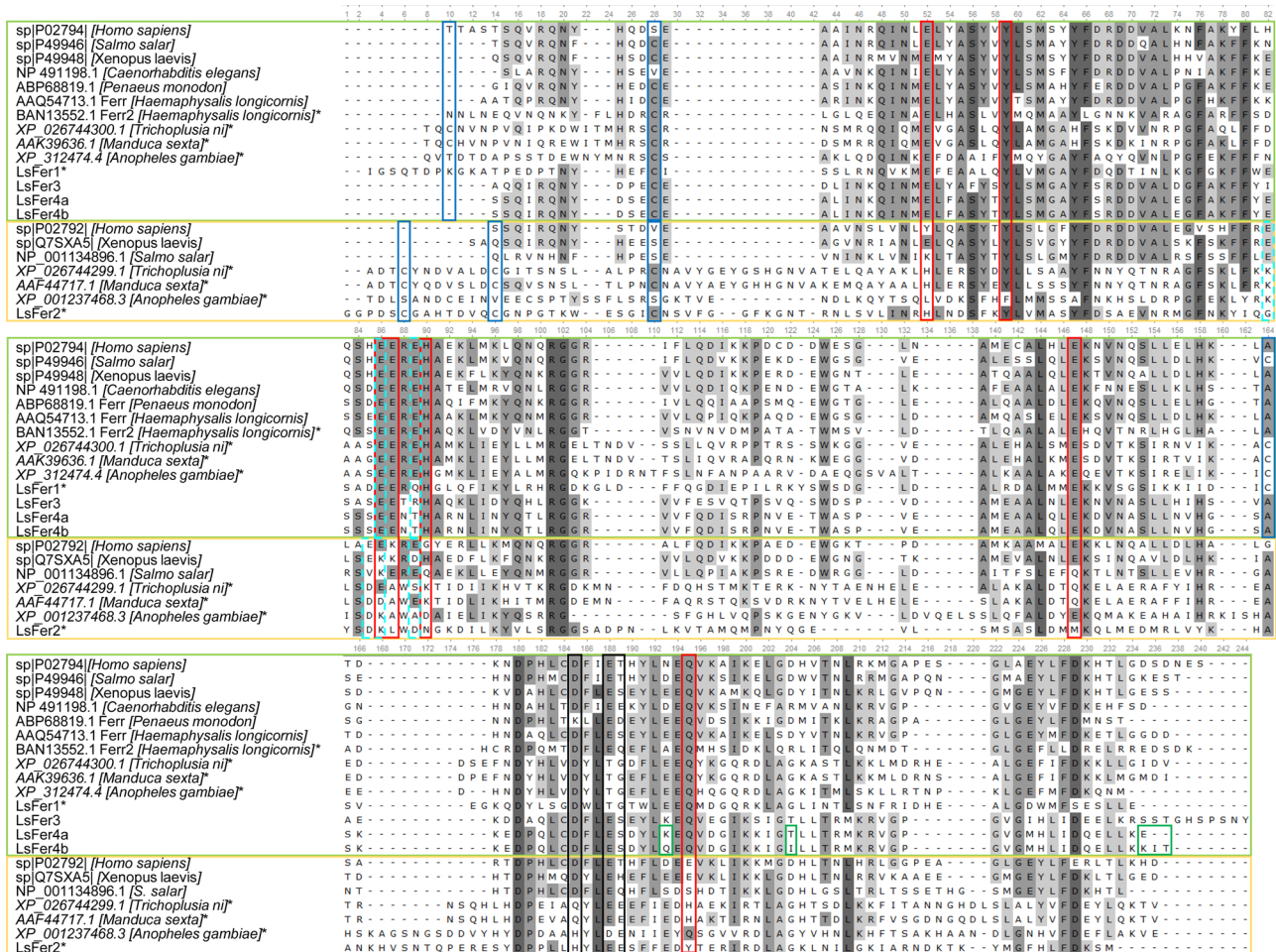


Fig. 1. Ferritin sequence alignment. Sequences found in *L. salmons* (LsFer1-4) with known ferritin sequences annotated as heavy (green outline) and light chain (yellow outline). Amino acids that make up the ferroxidase center of the heavy chain in human are marked with a red box, the conserved pore for iron entry black and the aa making up the human ferrihydrite nucleation center are marked with cyan (dashed line). The conserved cysteines, which are involved in inter and intra disulphide bridges in insects are marked with blue. Differences in the aa sequence between Fer4a and Fer4b are marked with green. Sequences with signal sequences are marked with*. For alignment, all signal sequences were removed. All other sequences were deleted for the start methionine.

in their intestine, this was not the case in the *LsFer1* and *LsFer2* knockdown animals (Table 3). In order to more closely examine the knockdown effects, sections were made for histology (Fig. 6). In the control louse (Fig. 6a), oocytes are stacked and well-structured with lipid-droplets (seen as white dots) and with chorions that define boundaries between individual oocytes. In the *LsFer1* knockdown animal, oocytes appear as a homogenous mash and without visible chorions subdividing individual oocytes (Fig. 6b). Histology of the *LsFer2* knockdown louse reveals a genital segment with little and highly under-developed oocytes present (Fig. 6c). Lice shown in Fig. 6 are representative of both experiments. Photographs of all lice from exp. 2 are shown in Supplementary Fig. S1.

The efficacies of the knockdowns of *LsFer1* and *LsFer2* were assessed by qPCR. Knockdowns were successful for both treatments in both experiments, and experiment 2 is presented with individuals' levels of transcripts (Fig. 7). In experiment 1, *LsFer1* is on average 85% down-regulated (Mann-Whitney U: $p = 0.008$, $n = 5$), and *LsFer2* is on average 78% down-regulated (t -test: $p = 0.005$, $n = 5$). In experiment 2, knockdown of *LsFer1* resulted in an on average 93% down-regulation (t -test: $p = 0.000171$, $n = 5$) (Fig. 7a). Knockdown of *LsFer2* resulted in a down-regulation of 60–86% for four out of five animals tested, whereas up-regulation of 41% was found in the last one (Fig. 7b). This individual had a similar phenotype and morphology as the rest of the knockdown group, and is therefore not omitted from the dataset or statistical analysis (Mann-Whitney U: $p = 0.076$, $n = 5$).

4. Discussion

In this study, we present the characterization and first functional studies of ferritin in the obligate hematophagous ectoparasitic salmon louse, *Lepeophtheirus salmonis*. We report the presence of four ferritin homologs (*LsFer1-4*) in the genome of the salmon louse, and find that two of these (*LsFer1-2*) have predicted signal peptides in the N-terminus of their aa sequences. Functional studies show that *LsFer1-2* are expressed in the midgut, and both are essential for the blood-feeding and reproduction of the adult female salmon louse.

Results from the sequence analysis tools used here give support to the hypothesis that *LsFer1-4* are homologs of ferritin as there are significant sequence similarities with ferritins of other species found by BLAST searches. Since *LsFer1,3* and *4* have the highly conserved motifs for the ferroxidase site, whereas *LsFer2* does not, *LsFer1,3* and *4* are likely heavy chain homologs (HCH), whereas *LsFer2* is likely a light chain homolog (LCH). This is further supported by the phylogenetic analysis, which shows that LsFer1 mainly clusters together with other HCHs and LsFer2 mainly with other LCHs (Fig. 2). LsFer3-4 clusters phylogenetically closer together with ferritin subunits without a signal peptide. Classically secreted ferritins are commonly found in arthropods where they are reported to be involved in detoxification, storage and distribution of iron. As a well-studied phenomenon in insects, ferritin is loaded with absorbed iron in the endoplasmic reticulum (ER), and is then secreted to the hemolymph, a tissue fluid analogous to

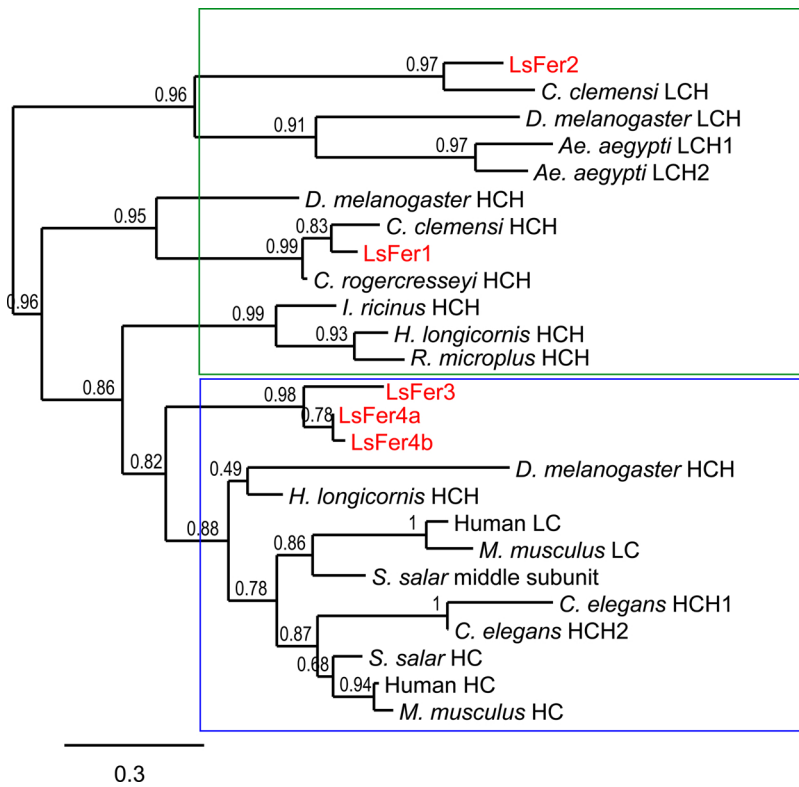


Fig. 2. Unrooted phylogenetic tree of vertebrate and invertebrate ferritin subunits. The phylogenetic analysis was performed on the Phylogeny.fr platform. Secreted ferritins are marked with the green box and intracellular ferritins with the blue box. Salmon louse ferritins (LsFer1-4) are written in red letters. LsFer1 clusters together with secreted invertebrate HCH ferritins, and LsFer2 clusters together with secreted invertebrate LCH ferritins. LsFer3-4 cluster together and are close to branches of intracellular heavy and light chain ferritins of both vertebrate and invertebrate origin. Numbers at branches represent support values (approximate likelihood-ratio). HC(H) = heavy chain (homolog), LC(H) = light chain (homolog). Scale bar: 0.3 amino acid substitutions per site.

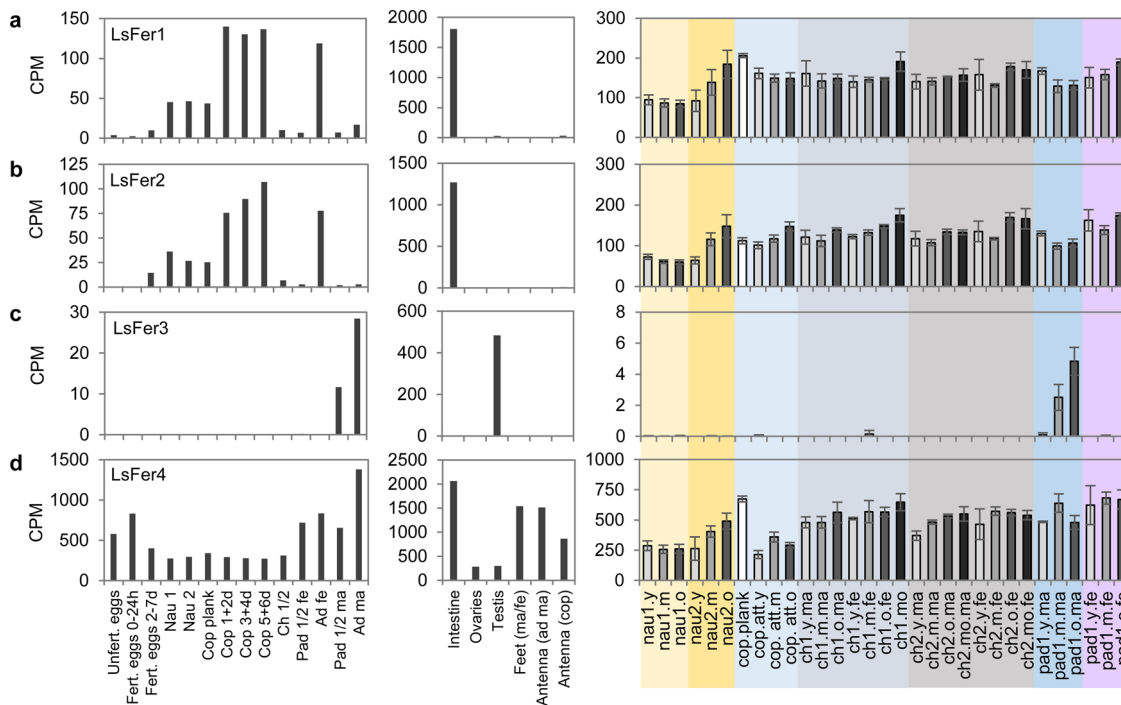


Fig. 3. Ontogeny. RNA-sequencing data (left and middle column: LiceBase, right column: Eichner et al., 2018 [28] with additional data from nauplius and attached copepodids (unpublished data)) for *LsFer1* (a), *LsFer2* (b), *LsFer3* (c) and *LsFer4* (d). Available reads were recounted for the transcribed regions of the ferritin genes found by RACE-PCR. See Section 2.4 “Ontogeny” for explanations of the abbreviations used in the figure.

blood in vertebrates, and subsequently used as a vehicle for iron transportation to various tissues [38]. In the current study, we find that both LsFer1-2 ferritin subunits are predicted to have signal peptides, and are thus likely destined for the secretory pathway. Since the salmon louse lacks the iron transfer protein transferrin (unpublished, <http://licebase.org>), it may utilize secreted ferritin to shuttle iron to recipient

tissues and still avoiding iron-related cytotoxicity. The localizations of the precursor and mature LsFer1-2 proteins are however not determined, as only transcript localization is assessed here. Further work is required to determine if ferritin acts as an iron transporter in the salmon louse. Also, whether LsFer1 and LsFer2 are subunits of the same protein, or if they make up two different proteins remains an

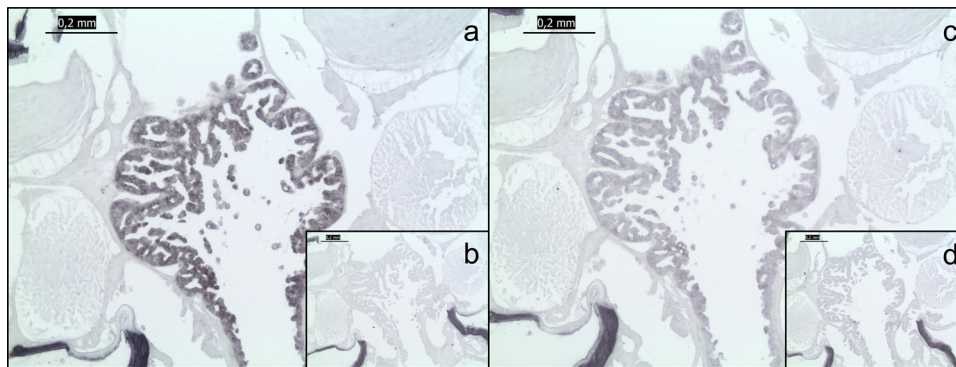


Fig. 4. *In situ* hybridization. The transcripts of both *LsFer1* (a) and *LsFer2* (c) are only found in cells lining the gut of *L. salmonis* by *in situ* hybridization. Negative controls (sense probes) of *LsFer1* (b) and *LsFer2* (d) show no signal.

unanswered question. Since *LsFer2* lacks conserved aa residues for ferroxidase catalytic activity, it is highly unlikely that the LCH subunit may constitute an iron storage molecule on its own. Also, *LsFer1* and *LsFer2* contain cysteine residues reported to form intersubunit disulfide bonds in other secretory ferritins [6].

Characterization of the *LsFer1-4* genes by RNA-Seq showed that *LsFer1-2* have similar expression patterns. Both secreted ferritin subunits are highly expressed in the intestine of the salmon louse, consistent with having an iron storage and/or transportation function. Additionally, *LsFer1-2* are expressed in the larval, non-feeding stages of the salmon louse, which could indicate extra functions of the ferritin subunits, or they could be necessary for detoxification of iron from the turnover of maternally derived iron-proteins. The similar expression patterns of *LsFer1-2* suggests that the two subunits could assemble into a complete ferritin shell. *LsFer3*, which is primarily expressed in testis, must have a male specific function. *LsFer4* has a more uniform expression pattern, and probably has an intracellular iron storage function in several tissues of the salmon louse. Further analysis by *in situ* hybridization confirmed that the transcripts of *LsFer1* and *LsFer2* are both expressed in cells lining the intestinal tract of the adult female salmon louse. Epithelial cells in the gut are the entry site for iron absorbed from the blood of the parasite's host, and is where iron storage proteins need to be ready and available. In the starvation experiment, the expression of *LsFer1-2* is decreasing with the increased starvation time. A reason for this could be that the salmon louse is an ectoparasite that is either on or off its host. It does not experience a gradient in iron availability, other than remnants of blood in the gut after feeding (seen as a fainter red color with increased starvation time). Expressing a nutrient storage molecule when there is an absence of nutrients available is unnecessary and requiring energy. Similar to our results, an HCH ferritin in *A. aegypti* was found in the midgut of the mosquito and was regulated by blood-feeding [39]. Also, Wu et al., found that a ferritin homolog in abalone *Haliotis discus hannai* was up-regulated by dietary iron [40]. Walter-Nuno et al., also found that blood-feeding increased the expression level of several genes involved in heme and iron metabolism, including ferritin [41]. These findings indicate that ferritin gene expression is a consequence of the dietary iron status. A common way of controlling ferritin transcript translation in a cell is by iron regulatory

Table 3

Overview of RNA interference knockdown experiments of *LsFer1* and *LsFer2*.

Experiment	Treatment	Animals recovered/ injected	Fully engorged ^a	Hatching success ^b
1	Control	19/39	19/19	19/19
	<i>LsFer1</i>	18/38	5/18	1/10
	<i>LsFer2</i>	23/39	10/23	5/10
2	Control	5/30	5/5	5/5
	<i>LsFer1</i>	12/30	0/12	0/6
	<i>LsFer2</i>	7/30	1/7	0/7

^a Determined by visual inspections of blood-filled intestines.

^b Number of successfully hatched egg string pairs and number of females bearing egg strings upon termination of the experiments.

proteins (IRPs) that inhibit ferritin translation during iron shortage by binding to an IRE upstream of the ferritin ORF [42]. Yet, no IREs were predicted in any of the ferritin sequences in the salmon louse, even though the louse does have an IRP-IRE complex [37]. We do not know if uptake of iron is controlling ferritin translation here as it does post-transcriptionally in vertebrates [43] and other various invertebrates [44,45]. Not all organisms depend on translational control by IRE however, e.g. plants regulate ferritin levels on a transcriptional level in response to iron and oxidants [46]. How ferritin expression is regulated in the salmon louse remains an unanswered question.

The functional study by knocking down *LsFer1* and *LsFer2* in the salmon louse mediated by RNAi had negative consequences for the fecundity of the parasite. Fewer of the adult female lice had egg strings, and when present, they had an overall much lower hatching success in both knockdown groups compared with the control group. Histological analyses demonstrated that oocyte development was impaired, and this is probably why eggs hatching was highly unsuccessful. Knockdown of genes involved in iron metabolism is already known to limit reproductive success of other hematophagous parasites, such as the tick's reproduction and development [44,47,48]. Furthermore, knockdown of a ferritin in the vector *Rhodnius prolixus* resulted in drastically reducing (95%) viable eggs for the hematophagous insect [41]. As the salmon louse is semi-transparent, its red, blood-filled gut can easily be observed

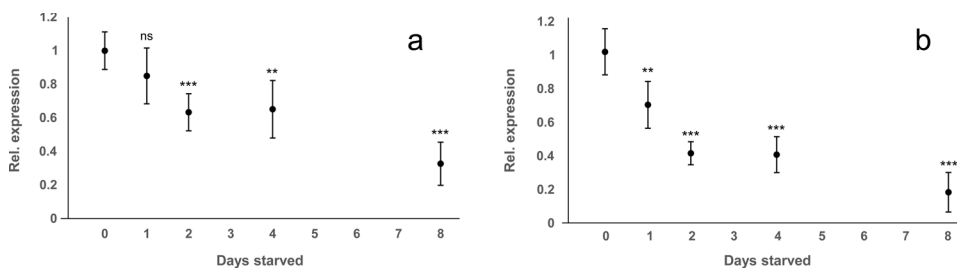


Fig. 5. Effect of starvation. Transcripts of both *LsFer1* (a) and *LsFer2* (b) were assessed in adult female lice by qPCR. The mRNA levels of both transcripts were calibrated against unstarved lice (day 0 post start of starvation), and showed increased down-regulation with increasing starvation time. Data are presented as mean values \pm SD. Asterisks indicate statistical significance against day 0: ** = $p \leq 0.01$, *** = $p \leq 0.0001$, ns = not significant. $n = 5$.

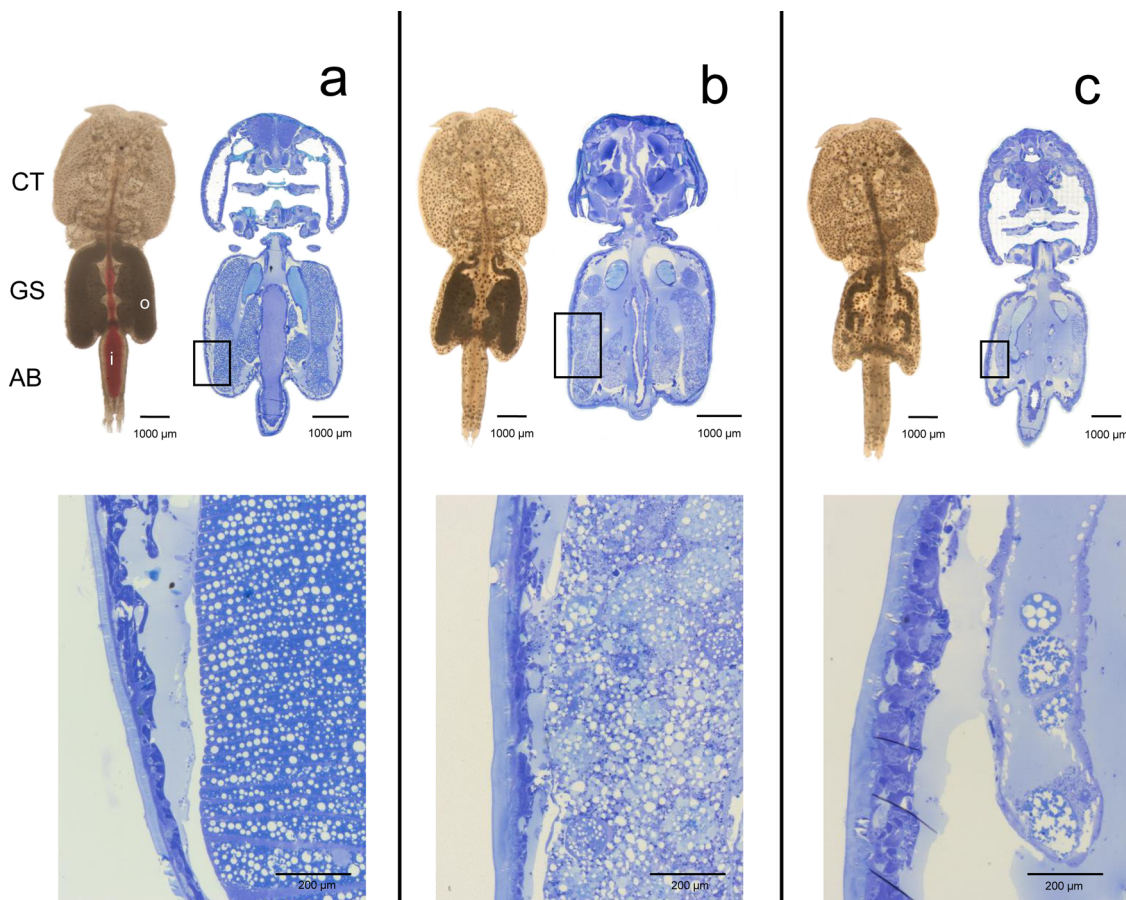


Fig. 6. Phenotype and histology. Phenotype and toluidine blue stained histological sections of an untreated control adult female louse (a), a *LsFer1* RNAi knockdown louse (b) and a *LsFer2* RNAi knockdown louse (c). Of every histological section, a magnified photo of the genital segment is shown in the lower panel. All three lice are representative of their group. CT = cephalothorax, GS = genital segment, AB = abdomen, i = intestine, o = oocyte.

by visual inspection. Animals in the knockdown group had less blood in their intestines than animals in the control group, which were fully engorged. This phenomenon has also been reported in ticks upon knockdown of ferritin [48]. An explanation for this could be as free iron generates ROS, having a reduced capacity of sequestering and thus detoxifying iron could lead to detrimental effects for the parasite upon blood-feeding. A solution for the salmon louse could be to cease the

blood-feeding behavior. Downstream effects of not ingesting blood would include severe undernutrition and consequently cause egg production to be halted.

In conclusion, this report on four ferritin homologs in the salmon louse is the first where we have functionally characterized the two secretory subunits (*LsFer1-2*). *LsFer1* and *LsFer2* were both found to be vital for blood-feeding and reproduction in the hematophagous parasite

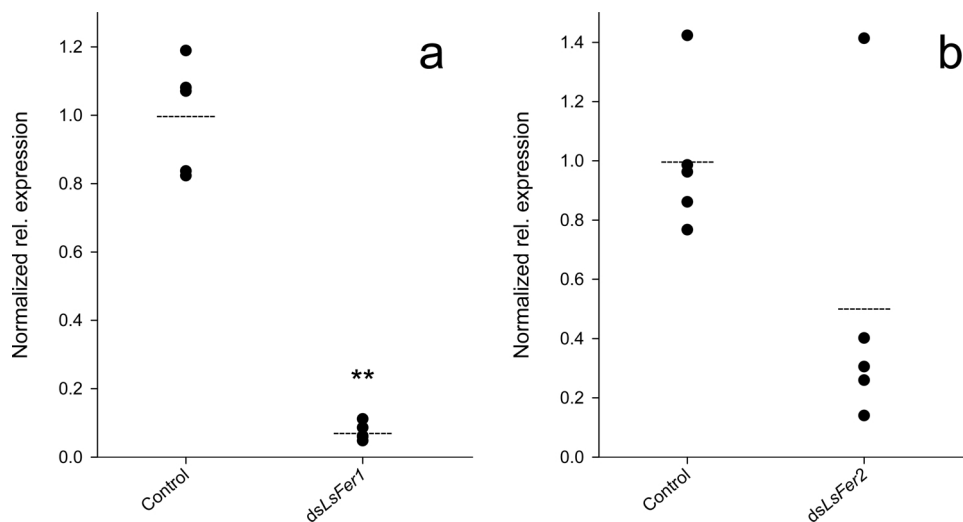


Fig. 7. Knockdown efficacy. RNAi mediated knockdown effect of (a) *LsFer1* and (b) *LsFer2* measured by qPCR from experiment 2. Results are displayed as individual animals' values, and the mean value for each group is indicated by a dotted line. ** = $p \leq 0.01$. $n = 5$.

in a knockdown study and starvation experiment. Our results confirm several previous findings on the importance of ferritin throughout arthropods. Further work on these genes and proteins could provide a deeper knowledge of the iron metabolism of *L. salmonis* and should be studied further. Considering the detrimental effects the knockdown of *LsFer1-2* had on the egg production in the salmon louse, these results could find their application as treatment targets in the aquaculture sector in order to combat the infamous parasite.

Funding

This research has been funded by The Research Council of Norway, SFI-Sea Lice Research Centre, grant number 203513/O30 and PreventT project, grant number 199778.

Declaration of Competing Interest

None.

Acknowledgements

We are grateful to Heidi Kongshaug, Per Gunnar Espedal, Lars Hamre, Bjørnar Skjold and Pavinee Nimmongkol for excellent help in the laboratories. The authors would also like to thank Dr. Michael Dondrup for helping with the analysis of the RNA-sequencing data.

Appendix A. Supplementary data

Supplementary material related to this article can be found, in the online version, at doi:<https://doi.org/10.1016/j.molbiopara.2019.111197>.

References

- J.L. Beard, Iron biology in immune function, muscle metabolism and neuronal functioning, *J. Nutr.* 131 (2001) 568–580.
- J. Emerit, C. Beaumont, F. Trivin, Iron metabolism, free radicals, and oxidative injury, *Biomed. Pharmacother.* 55 (2001) 333–339.
- E.G. Meyron-Holtz, S. Moshe-Belizowski, L.A. Cohen, A possible role for secreted ferritin in tissue iron distribution, *J. Neural Transm.* 118 (2011) 337–347, <https://doi.org/10.1007/s00702-011-0582-0>.
- P. Arosio, R. Ingrassia, P. Cavadini, Ferritins: a family of molecules for iron storage, antioxidant and more, *Biochim. Biophys. Acta* 1790 (2009) 589–599, <https://doi.org/10.1016/j.bbagen.2008.09.004>.
- D.Q.D. Pham, J.J. Winzerling, Insect ferritins: Typical or atypical? *Biochim. Biophys. Acta* 1800 (2010) 824–833, <https://doi.org/10.1016/j.bbagen.2010.03.004>.
- A.E. Hamburger, A.P. West, Z.A. Hamburger, P. Hamburger, P.J. Bjorkman, Crystal structure of a secreted insect ferritin reveals a symmetrical arrangement of heavy and light chains, *J. Mol. Biol.* 349 (2005) 558–569, <https://doi.org/10.1016/j.jmb.2005.03.074>.
- P. Ponka, Cellular iron metabolism, *Kidney Int.* 55 (1999) 2–11, <https://doi.org/10.1046/j.1523-1755.1999.055Suppl.69002.x>.
- P.O. Brandal, E. Egidius, I. Romslo, Host blood: A major food component for the parasitic copepod *Lepeophtheirus salmonis* Krøyeri, 1838 (Crustacea: caligidae), *Nor. J. Zool.* 24 (1976) 341–343.
- S.M. Aaen, K.O. Helgesen, M.J. Bakke, K. Kaur, T.E. Horsberg, Drug resistance in sea lice: a threat to salmonid aquaculture, *Trends Parasitol.* 31 (2015) 72–81, <https://doi.org/10.1016/j.pt.2014.12.006>.
- L.A. Hamre, C. Eichner, C.M.A. Caipang, S.T. Dalvin, J.E. Bron, F. Nilsen, G. Boxshall, R. Skern-Mauritzen, The salmon louse *Lepeophtheirus salmonis* (Copepoda: caligidae) life cycle has only two chalimus stages, *PLoS One* 8 (2013) 1–9, <https://doi.org/10.1371/journal.pone.0073539>.
- S.C. Johnson, L.J. Albright, The developmental stages of *Lepeophtheirus salmonis* (Krøyer, 1837) (Copepoda: caligidae), *Can. J. Zool.* 69 (1991) 929–950.
- S.C. Johnson, L.J. Albright, Development, growth, and survival of *Lepeophtheirus salmonis* (Copepoda: caligidae) under laboratory conditions, *J. Mar. Biol. Assoc. U.K.* 71 (1991) 425–436.
- C. Steentoft, S.Y. Vakhrushev, H.J. Joshi, Y. Kong, M.B. Vester-Christensen, K.T.-B. Schjoldager, K. Lavrsen, S. Dabelsteen, N.B. Pedersen, L. Marcos-Silva, R. Gupta, E.P. Bennett, U. Mandel, S. Brunak, H.H. Wandall, S.B. Levery, H. Clausen, Precision mapping of the human O-GalNAc glycoproteome through SimpleCell technology, *EMBO J.* 32 (2013) 1478–1488, <https://doi.org/10.1038/emboj.2013.79>.
- S.F. Altschul, W. Gish, W. Miller, E.W. Myers, D.J. Lipman, Basic local alignment search tool, *J. Mol. Biol.* 215 (1990) 403–410.
- P. Jones, D. Binns, H.-Y. Chang, M. Fraser, W. Li, C. McAnulla, H. McWilliam, J. Maslen, A. Mitchell, G. Nuka, S. Pesseat, A.F. Quinn, A. Sangrador-Vegas, M. Scheremetjew, S.-Y. Yong, R. Lopez, S. Hunter, Sequence analysis InterProScan 5: genome-scale protein function classification, *Bioinformatics.* 30 (2014) 1236–1240, <https://doi.org/10.1093/bioinformatics/btu031>.
- L. Käll, A. Krogh, E.L.L. Sonnhammer, A combined transmembrane topology and signal peptide prediction method, *J. Mol. Biol.* 338 (2004) 1027–1036, <https://doi.org/10.1016/j.jmb.2004.03.016>.
- M. Campillos, I. Cases, M.W. Hentze, M. Sanchez, SIREs: searching for iron-responsive elements, *Nucleic Acids Res.* 38 (2010) 360–367, <https://doi.org/10.1093/nar/gkq371>.
- The Uniprot Consortium, UniProt: a worldwide hub of protein knowledge, *Nucleic Acids Res.* 47 (2018) 506–515, <https://doi.org/10.1093/nar/gky1049>.
- K. Okonechnikov, O. Golosova, M. Fursov, Unipro UGENE: a unified bioinformatics toolkit, *Bioinformatics.* 28 (2012) 1166–1167, <https://doi.org/10.1093/bioinformatics/bts091>.
- R.C. Edgar, MUSCLE: multiple sequence alignment with high accuracy and high throughput, *Nucleic Acids Res.* 32 (2004) 1792–1797, <https://doi.org/10.1093/nar/gkh340>.
- A. Dereeper, V. Guignon, G. Blanc, S. Audic, S. Buffet, F. Chevenet, S. Guindon, V. Lefort, M. Lescot, O. Gascuel, Phylogeny.fr: robust phylogenetic analysis for the non-specialist, *Nucleic Acids Res.* 36 (2008) W465–W469, <https://doi.org/10.1093/nar/gkn180>.
- S. Guindon, O. Gascuel, A simple, fast, and accurate algorithm to estimate large phylogenies by maximum likelihood, *Syst. Biol.* 52 (2003) 696–704, <https://doi.org/10.1080/10635150390235520>.
- F. Chevenet, C. Brun, A.-L. Bañuls, B. Jacq, R. Christen, TreeDyn: towards dynamic graphics and annotations for analyses of trees, *BMC Bioinformatics* 7 (2006) 1–9, <https://doi.org/10.1186/1471-2105-7-439>.
- L.A. Hamre, K.A. Glover, F. Nilsen, Establishment and characterisation of salmon louse (*Lepeophtheirus salmonis* (Krøyer 1837)) laboratory strains, *Parasitol. Int.* 58 (2009) 451–460, <https://doi.org/10.1016/j.parint.2009.08.009>.
- L.A. Hamre, F. Nilsen, Individual fish tank arrays in studies of *Lepeophtheirus salmonis* and lice loss variability, *Dis. Aquat. Organ.* 97 (2011) 47–56, <https://doi.org/10.3354/dao02397>.
- T.D. Wu, C.K. Watanabe, GMAP: a genomic mapping and alignment program for mRNA and EST sequences, *Bioinformatics.* 21 (2005) 1859–1875, <https://doi.org/10.1093/bioinformatics/bti310>.
- Y. Liao, G.K. Smyth, W. Shi, featureCounts: an efficient general purpose program for assigning sequence reads to genomic features, *Bioinformatics.* 30 (2014) 923–930, <https://doi.org/10.1093/bioinformatics/btt656>.
- C. Eichner, M. Dondrup, F. Nilsen, RNA sequencing reveals distinct gene expression patterns during the development of parasitic larval stages of the salmon louse (*Lepeophtheirus salmonis*), *J. Fish Dis.* 41 (2018) 1005–1029, <https://doi.org/10.1111/jfd.12770>.
- M.D. Robinson, D.J. McCarthy, G.K. Smyth, edgeR: a Bioconductor package for differential expression analysis of digital gene expression data, *Bioinformatics.* 26 (2010) 139–140, <https://doi.org/10.1093/bioinformatics/btp616>.
- P. Frost, F. Nilsen, Validation of reference genes for transcription profiling in the salmon louse, *Lepeophtheirus salmonis*, by quantitative real-time PCR, *Vet. Parasitol.* 118 (2003) 169–174, <https://doi.org/10.1016/j.vetpar.2003.09.020>.
- A. Radonic, S. Thulke, I.M. Mackay, O. Landt, W. Siebert, A. Nitsche, Guideline to reference gene selection for quantitative real-time PCR, *Biochem. Biophys. Res. Commun.* 313 (2004) 856–862, <https://doi.org/10.1016/j.bbrc.2003.11.177>.
- M.W. Pfaffl, A new mathematical model for relative quantification in real-time RT-PCR, *Nucleic Acids Res.* 29 (2001) 16–21.
- S. Dalvin, P. Frost, E. Biering, L.A. Hamre, C. Eichner, B. Krossøy, F. Nilsen, Functional characterisation of the maternal yolk-associated protein (LsYAP) utilising systemic RNA interference in the salmon louse (*Lepeophtheirus salmonis*) (Crustacea: copepoda), *Int. J. Parasitol.* 39 (2009) 1407–1415, <https://doi.org/10.1016/j.ijpara.2009.04.004>.
- E.I. Heggland, C. Eichner, S.I. Støve, A. Martinez, F. Nilsen, M. Dondrup, A scavenger receptor B (CD36)-like protein is a potential mediator of intestinal heme absorption in the hematophagous ectoparasite *Lepeophtheirus salmonis*, *Sci. Rep.* 9 (2019) 1–14, <https://doi.org/10.1038/s41598-019-40590-x>.
- S. Dalvin, F. Nilsen, R. Skern-Mauritzen, Localization and transcription patterns of LsVasa, a molecular marker of germ cells in *Lepeophtheirus salmonis* (Krøyer), *J. Nat. Hist.* 47 (2013) 889–900, <https://doi.org/10.1080/00222933.2012.738830>.
- C. Tröfse, F. Nilsen, S. Dalvin, RNA interference mediated knockdown of the KDEL receptor and COPB2 inhibits digestion and reproduction in the parasitic copepod *Lepeophtheirus salmonis*, *Comp. Biochem. Physiol. Part B.* 170 (2014) 1–9, <https://doi.org/10.1016/j.cbpb.2013.12.006>.
- C. Tröfse, H. Kongshaug, M. Dondrup, F. Nilsen, Characterisation of iron regulatory protein 1A and 1B in the blood-feeding copepod *Lepeophtheirus salmonis*, *Exp. Parasitol.* 157 (2015) 1–11, <https://doi.org/10.1016/j.exppara.2015.06.010>.
- H. Nichol, J.H. Law, J.J. Winzerling, Iron metabolism in insects, *Annu. Rev. Entomol.* 47 (2002) 535–559.
- B.C. Dunkov, T. Georgieva, T. Yoshiga, M. Hall, J.H. Law, *Aedes aegypti* ferritin heavy chain homologue: feeding of iron or blood influences message levels, lengths and subunit abundance, *J. Insect Sci.* 2 (2002) 1–9.
- C. Wu, W. Zhang, K. Mai, W. Xu, X. Wang, H. Ma, Z. Liufu, Transcriptional up-regulation of a novel ferritin homolog in abalone *Haliotis discus hannai* Ino by dietary iron, *Comp. Biochem. Physiol. Part C.* 152 (2010) 424–432, <https://doi.org/10.1016/j.cbpc.2010.07.002>.
- A.B. Walter-Nuno, M.L. Taracena, R.D. Mesquita, P.L. Oliveira, G.O. Paiva-Silva, Silencing of iron and heme-related genes revealed a paramount role of iron in the

- physiology of the hematophagous vector *Rhodnius prolixus*, *Front. Genet.* 9 (2018) 1–21, <https://doi.org/10.3389/fgene.2018.00019>.
- [42] M.U. Muckenthaler, B. Galy, M.W. Hentze, Systemic iron homeostasis and the iron-responsive element/iron-regulatory protein (IRE/IRP) regulatory network, *Annu. Rev. Nutr.* 28 (2008) 197–213, <https://doi.org/10.1146/annurev.nutr.28.061807.155521>.
- [43] M.W. Hentze, S.W. Caughman, T.A. Rouault, J.G. Barriocanal, A. Dancis, J.B. Harford, R.D. Klausner, Identification of the iron-responsive element for the translational regulation of human ferritin mRNA, *Science* 238 (80-) (1987) 1570–1573, <https://doi.org/10.1126/science.3685996>.
- [44] O. Hajdusek, D. Sojka, P. Kopacek, V. Buresova, Z. Franta, I. Sauman, J. Winzerling, L. Grubhoffer, Knockdown of proteins involved in iron metabolism limits tick reproduction and development, *Proc. Natl. Acad. Sci. U. S. A.* 106 (2009) 1033–1038.
- [45] M. Muckenthaler, N. Gunkel, D. Frishman, A. Cyrklaff, P. Tomancak, M.W. Hentze, Iron-regulatory protein-1 (IRP-1) is highly conserved in two invertebrate species. Characterization of IRP-1 homologues in *Drosophila melanogaster* and *Caenorhabditis elegans*, *Eur. J. Biochem.* 254 (1998) 230–237.
- [46] J.-F. Briat, S. Lobréaux, N. Gringnon, G. Vansuyt, Regulation of plant ferritin synthesis: how and why, *Cell. Mol. Life Sci.* 56 (1999) 155–166.
- [47] R.L. Galay, R. Umemiya-Shirafuji, E.T. Bacolod, H. Maeda, K. Kusakisako, J. Koyama, N. Tsuji, M. Mochizuki, K. Fujisaki, T. Tanaka, Two kinds of ferritin protect ixodid ticks from iron overload and consequent oxidative stress, *PLoS One* 9 (2014), <https://doi.org/10.1371/journal.pone.0090661>.
- [48] R.L. Galay, K.M. Aung, R. Umemiya-Shirafuji, H. Maeda, T. Matsuo, H. Kawaguchi, N. Miyoshi, H. Suzuki, X. Xuan, M. Mochizuki, K. Fujisaki, T. Tanaka, Multiple ferritins are vital to successful blood feeding and reproduction of the hard tick *Haemaphysalis longicornis*, *J. Exp. Biol.* 216 (2013) 1905–1915, <https://doi.org/10.1242/jeb.081240>.